Available online at www.sciencedirect.com
ScienceDirect
Journal of Hazardous Materials 155 (2008) 369–377
Journal of Hazardous Materials
www.elsevier.com/locate/jhazmat

Preparation of nano-iron oxide red pigment powders by use of cyanided tailings

Li Dengxin *, Gao Guolong, Meng Fanling, Ji Chong

College of Environmental Science and Engineering, Donghua University, 2999 North Renmin Road, Songjiang District, Shanghai 201620, China

Received 8 August 2007; received in revised form 20 November 2007; accepted 20 November 2007
Available online 23 November 2007

Abstract

On one hand, cyanided tailings are one kind of pollutants. On the other hand, they contain a lot of valuable elements. So utilization of them can bring social and environmental benefits. In this paper, cyanided tailings were used to prepare nano-iron oxide red pigment powders by an ammonia process with urea as precipitant. At first, cyanided tailings were oxidized by nitric acid. Then, the oxidizing mixture was separated into solid and liquid parts. The liquid mixture was reduced by scrap iron and the impurity of it was removed by use of $NH_3{\cdot}H_2O$. Then, the seed crystal of γ-FeOOH was obtained, when the pure liquid reacted with ammonia liquid at the selected experimental conditions. At last, nano-iron oxide red pigment powders were prepared. The structure, morphology and size distribution of seed crystal and iron oxide red were characterized systematically by means of X-ray diffraction (XRD), transmission electron microscope (TEM) and laser particle size analyzer (LPSA). The results revealed that typical iron oxide nanoparticles were α-Fe_2O_3 with particle size of 50–70 nm. Furthermore, the factors that affected the hue and quality of the seed crystal and iron oxide red pigment were also discussed.
© 2007 Elsevier B.V. All rights reserved.

Keywords: Nano-iron oxide red; Pigment; Cyanided tailings; Nitric acid; Recycle

1. Introduction

Iron oxide red is technologically important materials and has superior character in non-toxicity, chemical stability, durability and low costs [1]. It is widely applied as components in various industrial products, e.g., pigments in the building industry, inorganic dyes, ceramics, pigments and adsorbents in the paper industry, lacquers or plastics [2–4].

There are many methods reported for the preparation of iron oxide red, e.g. dry methods and wet methods. Wet methods include nitric acid oxidation, sulphuric acid oxidation, and ammonia process, et al. [5]. Ammonia process uses ferrous sulfate as material instead of sheet iron. So the process has advantages in saving metal resources and protecting the environment. On one hand, cyanided tailings are one kind of pollutants. On the other hand, they contain a lot of valuable elements. So utilization of them can bring social and environmental benefits [6]. However, there is not much research on the iron oxide red preparation by cyanided tailings.

In the present study, an attempt has been made to prepare nano-iron red oxide pigment by cyanided tailings via an ammonia process with urea as the precipitant. The factors that influenced characters of seed crystal and iron oxide red were discussed. The result shows that nano-iron oxide red could be prepared with cyanided tailings under suitable conditions. The quality of the product can meet the first rank criterion of GB1863-89 (China Industrial Standard).

2. Experimental

2.1. Materials and reagents

All reagents used in this study were of analytical grade and locally procured. The cyanided tailings used in the experiment were obtained from Penglai Gold Smelting Plant in Shandong Province, China. Table 1 shows its chemical composition.

* Corresponding author. Tel.: +86 21 677 92541; fax: +86 21 677 92522.
E-mail addresses: lidengxin@dhu.edu.cn, clidx@yahoo.com (L. Dengxin).

0304-3894/$ – see front matter © 2007 Elsevier B.V. All rights reserved.
doi:10.1016/j.jhazmat.2007.11.070

Table 1
Chemical analysis of the cyanided tailings

Element	Content
Au (g/t)	3.6
Ag (g/t)	25.0
Cu (%)	0.21
Pb (%)	0.42
Zn (%)	0.64
S (%)	41.22
As (%)	0.42
Si (%)	3.73
Al (%)	1.24
Fe (%)	38.07

2.2. Nitric acid oxidation of cyanided tailings

The schematic diagram of facility for the cyanided tailings pretreatment is shown in Fig. 1. This experimental facility mainly consists of a fluidized bed, a catalyst regeneration setting and oxidized solution comprehensive utilization unit. The fluidized bed is a quartz cylinder with 100 mm i.d. and 2500 mm high. In the bottom of the fluidized bed, there is a gas distributor. Before starting an experiment, the fluidized bed was fluidized by oxygen and preheated to the desired operation temperature. The superficial velocity can be kept at the desired value. Cyanided tailings was mixed with certain amount of hot water and stirred for about 10 min. Then, the sludge was sprayed into hot fluidized bed reactor. Oxygen or air in NO_x regeneration setting mixed, was injected into the fluidized bed via the gas distributor, and reacted with the sludge.

The oxidized tailings were discharged out in the precipitation section outlet, and were separated into solid and liquid parts in cyclone centrifugal separator. Then, partial liquid mixed with the new sludge and reflowed into fluidized bed reactor, while the catalyst entered into regeneration setting for recycling. The remainder was used to prepare nano-iron oxide red and oxidized tailings were used to leach valuable metals.

Table 2
Experimental parameters of seed crystal preparation for different cases

No.	Volume (mL)	pH	Amount of air (m^3/h)	Temperature (°C)	Fe^{2+} (g/L)
1	300	9–10	0.1		20
2	300		0.1	15	20
3	300	9–10		15	20
4	300	9–10	0.1	15	
5	300	9–10	0.1	15	20

2.3. Purification of oxidized liquid

Scrap iron was added to the above oxidized solution before filtration. After scrap iron reacted completely with the oxidized liquid, the reduced mixture was filtered. Ammonia ($NH_3{\cdot}H_2O$) was added dropwise to the filtrate until pH reached 4–5 to purify ferrous sulfate in order to remove As, Pb, Si, Al, et al. The obtained pure solution was used to prepare seed crystal and the filter residues could be used to leach valuable metals.

2.4. Preparation of seed crystal

Twenty-five percent $NH_3{\cdot}H_2O$ solution was added dropwise to the purified solution until the pH of reaction system reached a certain degree. Then, air was bubbled into the mixture for a certain time at preset temperature. The resulting red orange solid product was then used as the seed crystal for the preparation of hematite. The reaction processes are as follows:

$$2NH_4OH + FeSO_4 \rightarrow Fe(OH)_2\downarrow + (NH_4)_2SO_4 \quad (1)$$

$$4Fe(OH)_2 + O_2 \rightarrow 4\gamma\text{-}FeOOH \downarrow + 2H_2O \quad (2)$$

Table 2 shows the experimental parameters of seed crystal preparation for different cases.

The effect of addition order of dispersant on the quality of seed crystal was discussed. Tartaric acid with 1% amount of

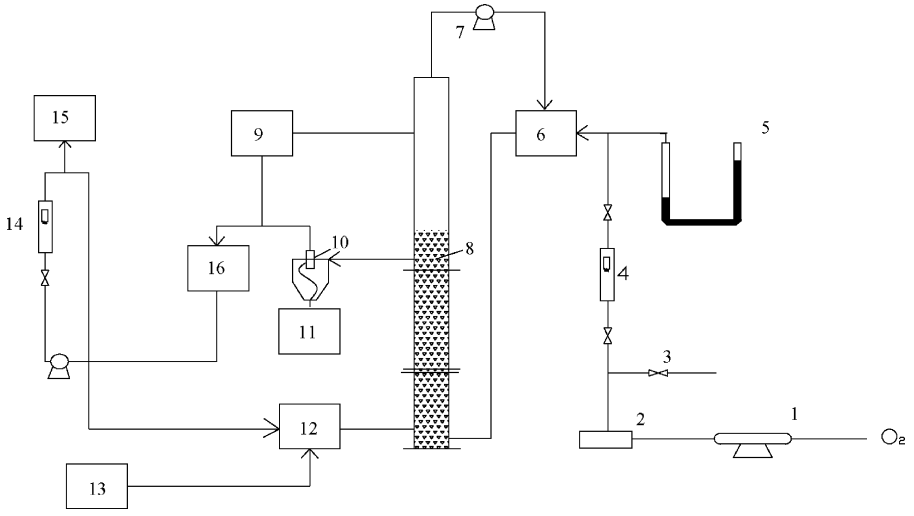

Fig. 1. Schematic pretreatment process of cyanided tailings: (1) air compressor; (2) buffer; (3) valve; (4) gas flow meter; (5) differential gage; (6) catalyst regeneration setting; (7) air compressor; (8) three-phase fluidized bed; (9) pressure probe; (10) hydraulic cyclone; (11) tailings; (12) stirred tank reactor; (13) cyanided tailings; (14) liquid flow meter; (15) oxidized solution comprehensive utilization unit; (16) strainer.

ferrous sulfate was chosen as the dispersant. With other experimental conditions fixed as listed in Table 2 (case 5), three different feeding orders were taken as follows: one method was that the dispersant was added into seed mixture after the end of preparation reaction for the seed crystal; another method was that the dispersant was added into seed mixture before adjusting pH of the mixture for preparation seed crystal, and the last one was that the dispersant was added into seed mixture after adjusting pH.

2.5. Preparation of hematite (α-Fe_2O_3)

The above pure ferrous sulfide solution was heated by water bath up to a certain temperature. Urea, the seed crystal and ferrous sulfate were added to the mixture and the pH of the mixture was adjusted to 3–4. Then, the air was bubbled into the mixture. After ageing at known temperature for a defined period of time, sodium dodecyl benzene sulfonate (SDBS) with 1% amount of ferrous sulfate was added and stirred for 1 h. The resulting precipitate was filtered off and washed with distilled water and allowed to dry at room temperature. The obtained product was characterized by X-ray powder diffraction (XRD) and transmission electron microscope (TEM).

The main reactions are as follows:

$$H_2NCONH_2 + H_2O \rightarrow CO_2\uparrow + 2NH_3 \quad (3)$$

$$NH_3 + H_2O \rightarrow NH_4OH \quad (4)$$

$$4FeSO_4 + O_2 + 6H_2O \rightarrow 4\gamma\text{-}FeOOH \downarrow + 4H_2SO_4 \quad (5)$$

$$H_2SO_4 + 2NH_4OH \rightarrow (NH_4)_2SO_4 + 2H_2O \quad (6)$$

$$2\gamma\text{-}FeOOH \rightarrow 2\alpha\text{-}Fe_2O_3\downarrow + H_2O \quad (7)$$

On the other hand, the effects of experimental factors including temperature, pH, velocity of air flow, concentration of ferrous sulfate and SDBS on the iron oxide red and the optimum molar ratio of urea and ferrous sulfate were also investigated. Table 3 shows the experimental parameters of iron oxide red preparation for different cases.

2.6. Analysis method

2.6.1. Titration of iron ion

Chemical analysis of the liquids was performed to estimate the ferrous and ferric iron content by a titration method according to GB 1863-89 (China Industrial Standard). The results were the mean values of the two experiments using the same sample.

2.6.2. Transmission electron microscope (TEM)

The size and morphology of iron oxide nanoparticles were observed by TEM (JEM-1230, JEOL, Japan). The sample for TEM analysis was obtained by placing a drop of dispersant onto a carbon coated copper grid without any staining, and drying it in air at room temperature.

2.6.3. X-ray diffraction (XRD)

The X-ray diffraction (XRD) analyses were performed using a Cu Kα (1.5418 A) source (40 KV, 40 mA) from Siemens D-501, with a graphite secondary monochromator and a scintillation counter detector. The powered sample was placed on a flat plastic plate, which was rotated at 30 rpm. The scans were performed at 25 °C in steps of 0.04 °C, with a recording time of 2 s for each step. Where accurate 2θ values were required, Si was added as an internal 2θ standard.

2.6.4. Laser particle size analyzer (LPSA)

Laser particle size analyzer (LS 13 320) was used to analyze the size distribution of the obtained particles.

2.7. Calculation of ferrous ion conversion rate

$$C_r = \frac{W_1 - W_2}{W_1} \quad (8)$$

where C_r is the conversion rate of ferrous ion; W_1 is weight of original ferrous ion; W_2 is weight of unreacted ferrous ion in the reaction system.

3. Result and discussion

3.1. Nitric acid oxidation of cyanided tailings

In order to find the optimum oxidation conditions in the course of pretreatment of cyanided tailings, three important factors were selected including initial temperature of oxidization, initial concentration of nitric acid and mass ratio of nitric acid and cyanided tailings (MRNACT) and orthogonal experiment as shown in Table 4 was conducted. From Table 4, it is obvious that the optimum factors of oxidation of cyanided tailings are as follows: reaction temperature is 80 °C; initial concentration of nitric acid is 30%; MRNACT is 3:1. Under these conditions, oxidation rate is 90.06% and pyrite in tailings has been oxygenated efficiently. Oxidation sludge can be delivered to leaching gold.

3.2. Purification of oxidized liquid

In order to find the optimum purification conditions, three important factors were selected including reaction temperature,

Table 3
Experimental parameters of iron oxide red preparation for different cases

No.	Volume(mL)	pH	Amount of air (m^3/h)	Temperature (°C)	$[H_2NCONH_2]/[Fe^{2+}]$
1	300	3–4	0.14		3.5:1
2	300		0.14	80–85	3.5:1
3	300	3–4		80–85	3.5:1

Table 4
Orthogonal experiment of cyanided tailings oxidized by nitric acid

No.	Factor		
	Reaction temperature	Initial concentration of nitric acid	Feed proportion of nitric acid and cyanided tailings
1	20	10	1
2	20	20	2
3	20	30	3
4	50	10	2
5	50	20	3
6	50	30	1
7	80	10	3
8	80	20	1
9	80	30	2
K_1	60	63.7	29.2
K_2	66.3	76.3	76.8
K_3	76.2	90.8	90.6

reaction time and M_{Fe}:M_{Fe3+} (M_{Fe3+} expresses ferric ion's mass of oxidization filtrate) and orthogonal experiment as shown in Table 5 was conducted. From Table 5, it can be found that the optimum purification conditions of oxidized liquid are as follows: reaction temperature is 40 °C; reaction time is 60 min; M_{Fe}:M_{Fe3+} is 1:1. Under the optimum conditions, conversion ratio of ferric ion is 100%; rate of displacement of copper is 91.2%; rate of displacement of silver is 96.9%; arsenic and lead have been removed and pure ferrous sulfate solution can be obtained.

3.3. Preparation of seed crystal

3.3.1. Effect of temperature on the quality of seed crystal

To study the effect of temperature, a series of experiments were performed with the temperature ranging from 15 to 45 °C. Other experimental parameters are listed in Table 2 (case 1). Because temperature can promote the oxidizing reaction of ferrous sulfate, C_r tends to be high with the rise of temperature as shown in Fig. 2(a). When ferrous sulfate is oxidized at 45 °C, C_r is 97%, while C_r is only 93% when ferrous sulfate is oxidized at 15 °C.

Table 5
Orthogonal experiment of purification of reaction mixture

No.	Factor		
	Reaction temperature	Reaction time	M_{Fe}:M_{Fe3+}
1	20	30	0.2
2	20	60	0.6
3	20	90	1.0
4	40	30	0.6
5	40	60	1.0
6	40	90	0.2
7	60	30	1.0
8	60	60	0.2
9	60	90	0.6
K_1	94	96	22
K_2	99	100	80
K_3	98	100	96

The crystallinity of the crystals produced, both in terms of foreign metal impurities and crystal phase, is an important feature which results in different chroma and hue of the pigment. The different phases of iron oxide have different hues. Table 6 shows the color change of seed crystal prepared at different temperatures. It is obvious that the temperature has an obvious effect on the chroma of seed crystal. The color of the seed crystal grows darker with reaction temperature increasing. At lower temperature, the color of the seed crystal is bright red brown, while the color of the seed crystal changes into black at 45 °C. The latter seed crystal can not grow into red iron oxide particles because it is not an iron oxide red seed crystal proved by its XRD pattern as shown in Fig. 3.

Fig. 3 shows the XRD patterns of the seed crystal prepared at different temperatures. It is observed that XRD patterns have obvious diffraction peaks, indicating that they have the highly crystalline character of the iron oxide. The XRD patterns shows

Table 6
Color of seed crystal prepared on different conditions

Factors	Color
Temperature (°C)	
15	Turkey red brown
25	Red brown
35	Dark red brown
45	Black
pH	
8–9	Jacinth
9–10	Red brown
10–11	Deeper red brown
>11	Dark brown
Air (m^3/h)	
0.04	Black
0.1	Turkey red brown
0.14	Red brown
0.2	Dark red brown
$FeSO_4$ (g/L)	
10	Red brown
20	Red brown
30	Dark red brown
40	Black

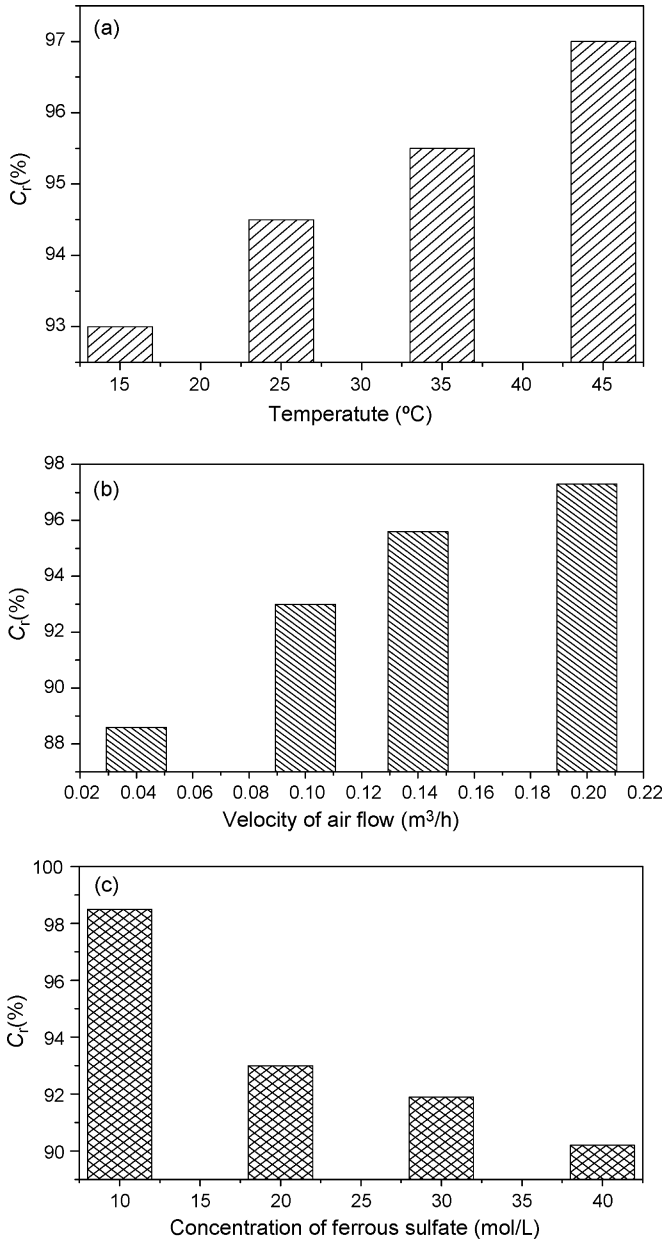

Fig. 2. Effect of different conditions on the conversation rate of Fe^{2+}. (a) Effect of temperature on the conversation rate of Fe^{2+} (volume: 300 mL; pH 9–10; velocity of air flow: 0.1 m^3/h; concentration of ferrous sulfate: 20 g/L); (b) effect of velocity of air flow on the conversation rate of Fe^{2+} (volume: 300 mL; pH, 9–10; T: 15 °C; concentration of ferrous sulfate, 20 g/L); (c) Effect of concentration of ferrous sulfate on the conversation rate of Fe^{2+} (volume, 300 mL; pH: 9–10; velocity of air flow, 0.1 m^3/h).

that the peaks of the seed crystal prepared at 15 °C are broader than those of the seed crystal prepared at 45 °C. According to the formula of Sreeram [7], with other conditions fixed, the width of diffraction peak is inversely proportional to the size of the particle. So it can be concluded that the grain size of seed crystal prepared at low temperature is greatly less than that of seed crystal prepared at high temperature. While the XRD pattern of the seed crystal prepared at 15 °C matches well with the standard γ-FeOOH reflections, the XRD pattern of the seed crystal prepared at 45 °C can be assigned to the Fe_3O_4 phase. It is obvious that crystal seed changes from γ-FeOOH to Fe_3O_4 with the rise of reaction temperature. Therefore, the optimum reaction temperature is 15 °C.

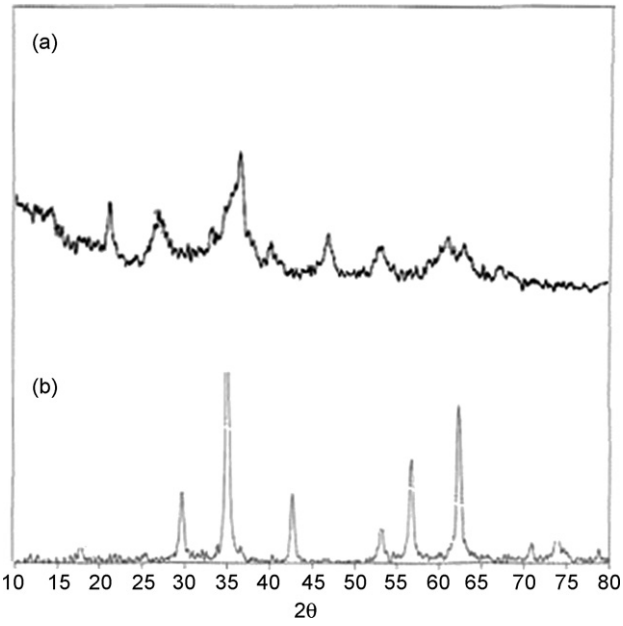

Fig. 3. XRD patterns of the seed crystal at different temperatures (a: 15 °C; b: 45 °C).

3.3.2. *Effect of pH on the quality of seed crystal*

To study the effect of pH, the sample was subjected to different pH of 8–9, 9–10, 10–11. Other parameters are listed in Table 2 (case 2). The results presented in Table 6 indicate that the color of seed crystal grows darker with the increase of pH and pH of 9–10 is favored for achieving a monodisperse character.

Fig. 4 shows the XRD pattern of the seed crystal prepared at pH of 8–9. The XRD pattern has obvious diffraction peaks, indicating that it has highly crystal structure. It matches well with the standard δ-FeOOH reflections. In the process of preparing iron oxide red, the seed crystal prepared at pH of 8–9 grows into iron oxide yellow, while the seed crystal prepared at pH of 9–10 grows into iron oxide red. This implies the optimum pH

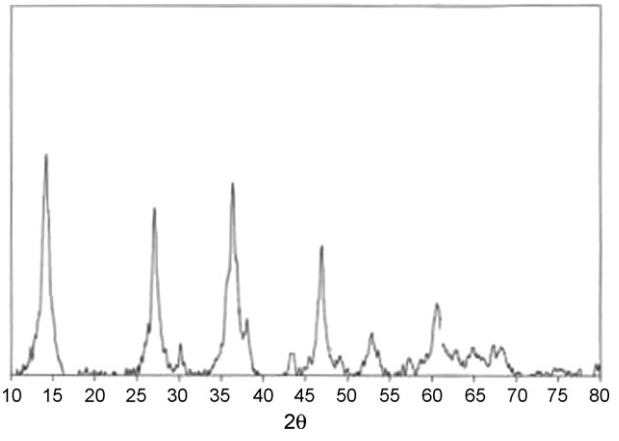

Fig. 4. XRD pattern of seed crystal prepared at pH of 8–9.

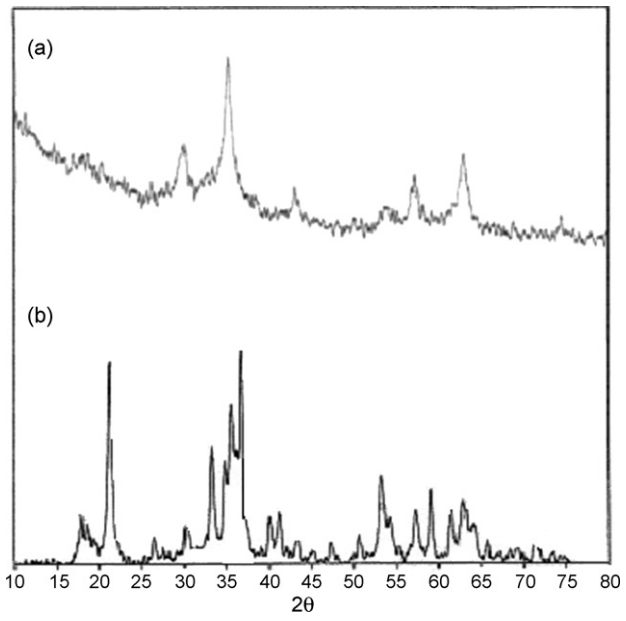

Fig. 5. XRD pattern of seed crystal prepared at different velocities of air flow (a) 0.1 m^3/h; (b) 0.04 m^3/h.

is 9–10 in the process of preparing seed crystal. Either higher or lower pH can have drastic influence on the preparation of red iron oxide.

3.3.3. Effect of velocity of air flow on the quality of seed crystal

To study the effect of velocity of air flow, a series of experiments were performed at different velocities of air flow ranging from 0.04 to 0.2 m^3/h. Other parameters are listed in Table 2 (case 3).

The effect of velocity of air flow on C_r is given in Fig. 2(b). As can be seen from Fig. 2(b), C_r increases with the increase of velocity of air flow. At the velocity of 0.04 m^3/h, C_r is only 88.4%, While C_r is high up to 97.3% at the velocity of 0.20 m^3/h. This indicates that air flow can promote the reaction. When the air flow velocity is higher, dissolved oxygen increases and more Fe^{2+} converts into seed crystal.

Table 6 shows color of seed crystal prepared at different velocities of air flow. The color of seed crystal changes gradually from black to red brown with the increase of velocity of air flow, but the color of seed crystal changes from bright red brown to dark red brown at excessive velocity of air.

Fig. 5 shows the XRD patterns of the seed crystal prepared at different velocities of air flow. The XRD patterns have obvious diffraction maximum, indicating that they had highly crystal structure. The former XRD pattern matches well with the standard γ-FeOOH reflections, while the latter can be assigned to the Fe_3O_4 phase. According to the analysis of phase, the seed crystal of iron oxide black will form when the velocity of air flow is small. The main possibility is: the velocity of $Fe(OH)_2$ being oxidized into Fe_2O_3 is low with little amount of air, and Fe $(OH)_2$ maybe reacts with the formed Fe_2O_3 into nucleus of Fe_3O_4 crystallization prior to its oxidization into Fe_2O_3. At excessively high velocity of air flow, formed seed crystal is still γ-FeOOH. But its color is dark, mainly because many formed crystal nucleus rubbed mutually at great velocity of air and their ability of reflecting light decreases. Therefore, the optimum velocity of air flow is 0.1 m^3/h.

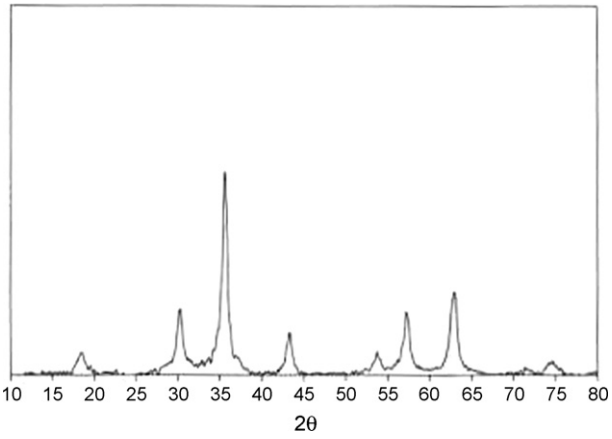

Fig. 6. XRD pattern of the seed crystal prepared at high concentration of ferrous sulfate.

3.3.4. Effect of concentration of ferrous sulfate on the quality of seed crystal

To study the effect of concentration of ferrous sulfate, a series of experiments were performed with the concentration ranging from 10 to 40 g/L. Other parameters are listed in Table 2 (case 4).

Fig. 2(c) shows the influence of concentration of ferrous sulfate on C_r. C_r decreases with the rise of concentration of ferrous sulfate. When the concentration of ferrous sulfate is 10 g/L, C_r is high up to 98.5%. While for a 40 g/L ferrous sulfate concentration, C_r is only 90.2%.

Table 6 shows the color of seed crystal prepared at different concentrations of ferrous sulfate. The color of seed crystal changes from red brown to black with the concentration of ferrous sulfate increasing.

Fig. 6 shows the XRD pattern of the seed crystal prepared at high concentration of ferrous sulfate. The XRD pattern has obvious diffraction maximum, indicating that it has highly crystal structure. It matches well with the standard Fe_3O_4 reflections. It demonstrates that the phase of seed crystal changes with the concentration of ferrous sulfate increasing and the seed crystal cannot be used to prepare iron oxide red pigment. Ferrous sulfate with low concentration can be used to prepare seed crystal, but when the concentration of ferrous sulfate is excessively low, the producing velocity of crystal nucleus is less than its growing velocity and the obtained grain size is big, so it can influence the characteristic of iron oxide red pigment. Therefore, the optimal concentration of ferrous sulfate in the process of seed crystal preparation is 20 g/L.

3.3.5. Effect of addition order of dispersant on the quality of seed crystal

The sedimentation time by the three addition orders of dispersant separately were measured as shown in Fig. 7. Fig. 7 indicates when tartaric acid (dispersion) is added after adjusting

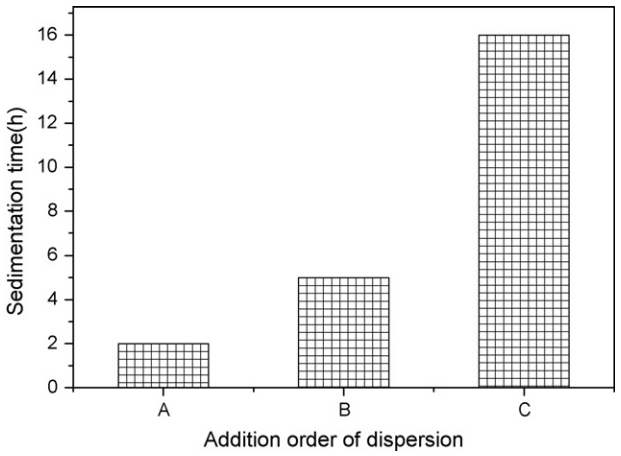

Fig. 7. Effect of addition order of dispersion on the sedimentation time of suspension: (A) added after complete reaction; (B) added before adjusting pH; (C) added after adjusting pH.

Table 7
Color of iron oxide red prepared on different conditions

Factor	Color
Temperature (°C)	
60–65	Yellow
70–75	Jacinth
80–85	Turkey red
90–95	Mauve
pH	
2–3	Yellow
3–4	Turkey red
4–5	Mauve
5–6	Dark red
Air (m^3/h)	
0.08	Dark red
0.14	Turkey red
0.20	Yellow

pH, the sedimentation time of seed crystal is the longest and the third addition method is the best to prepare seed crystal.

The dispersion has a drastic effect on the size distribution of iron oxide nanoparticles in this work as shown in Fig. 8. It can be found that dispersion can disperse the crystal nucleus, avoid its agglomerating and make it more regular.

3.4. Preparation of iron oxide red

3.4.1. Effect of temperature on the character of iron oxide

To study the effect of temperature on the character of iron oxide red, a series of experiments were performed with the temperature ranging from 60 to 95 °C. Other parameters are listed in Table 3 (case 1).

As shown in Table 7, the color of the resulting products gives the following shade as the temperature increases: yellow, jacinth, Turkey red and mauve. This is mainly because there is γ-FeOOH dehydration process and it has close correlation with temperature. Dehydration process speeds up with the rise of temperature. The obtained seed crystal is red with light yellow, because it contains partial water of crystallization under 70–75 °C. Dehydration is very prompt and the obtained seed crystal is bright under higher temperature. If the reaction temperature maintains excessively high, the velocity of γ-FeOOH dehydration speeds up and the oxidization period shortens. So the color of resulting products is red with purple. Therefore, the optimum temperature in the process of preparation of iron oxide red is 80–85 °C.

3.4.2. Effect of pH on the character of iron oxide

To study the effect of pH on the character of iron oxide red, a series of experiments were performed at different pH of 2–3, 3–4, 4–5, and 5–6. Other parameters are listed in Table 3 (case 2).

It was observed that the color of the resulting products grows from yellow to red with pH increasing. At pH of 2–3, the result-

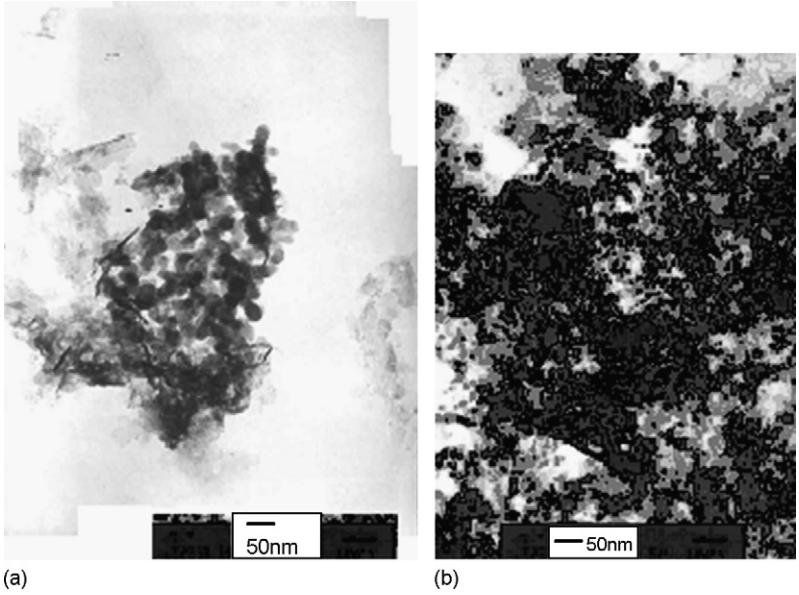

Fig. 8. TEM of seed crystal: (a) added dispersion; (b) no added dispersion.

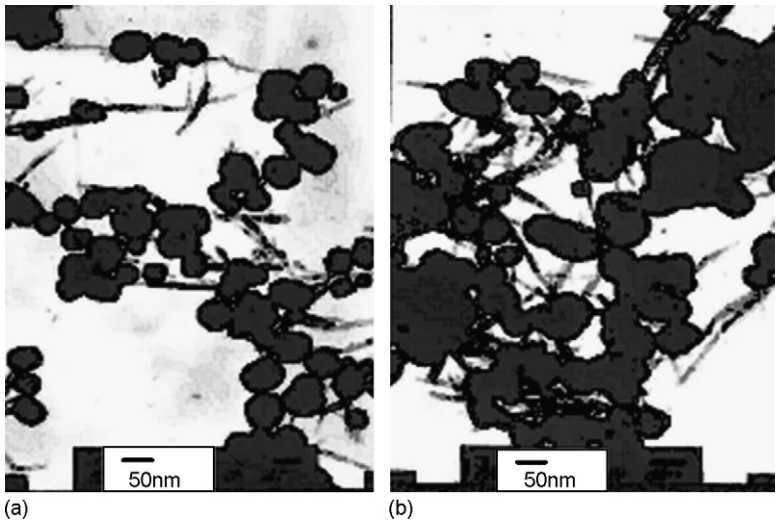

Fig. 9. TEM of iron oxide red (a) added SDBS; (b) no added SDBS.

ing product is iron oxide yellow, while, at pH of 3–4, the resulting product is bright iron oxide red. When pH > 4, the color of the obtained iron oxide red is little darker. Therefore, the optimum pH is 3–4.

3.4.3. Effect of velocity of air flow on the character of iron oxide red

To study the effect of velocity of air flow, a series of experiments were performed at different velocity of air flow ranging from 0.08 to 0.20 m^3/h. Other parameters are listed in Table 3 (case 3). Table 7 shows the color of the resulting product prepared at different velocities of air flow. The color of the resulting product grows from deeper to shallow as the velocity of air flow increases. When the velocity of air flow is 0.2 m^3/h, the resulting product is not iron oxide red but iron oxide yellow. This is mainly because there is close relationship between the oxidization velocity of ferrous sulfate and amount of air. At low velocity of air flow, ferrous sulfate is oxidized slowly and urea reacts with it to be $Fe(OH)_2$. So the color of iron oxide red is influenced and becomes deeper. At high velocity of air flow, ferrous sulfate is oxidized excessively fast and the formed FeOOH has not enough time to dehydrate. So the resulting product is not iron oxide red but iron oxide yellow. Therefore, the velocity of air flow must have a proper scope. According to the experiments, the optimal velocity of air flow is 0.14 m^3/h.

3.4.4. Optimum molar ratio of urea and ferrous sulfate

The dosage of ferrous sulfate can be decided from hue change of iron oxide red and the fact that the particle size of crystal nucleus is several nanometers to dozens of nanometers as shown in the process of seed crystal preparation.

Table 8 shows solution actuality at different molar ratios of urea and ferrous sulfate (MRUFS). Under different MRUFS, the pH of the mixture for preparing iron oxide red is different. The reason is that the OH^- from the urea hydrolysis can neutralize with H^+ by the ferric ion hydrolysis. When MRUFS is 3.5:1, the pH of the mixture for preparing iron oxide red is 3–4 and the color of the mixture become red. Under these conditions, the color of the resulting product (iron oxide red) is Turkey red. Thus the optimum MRUFS is 3.5:1.

Table 8
Solution actuality at different molar ratios of urea and ferrous sulfate

MRUFS	Solution actuality
1:1	pH is about 2; the color of solution grows yellow
2:1	pH is 2–3; the color of solution grows yellow
3.5:1	pH is 3–4; the color of solution grows from red brown to red
5:1	pH increases gradually; the color of solution grows black

3.4.5. Effect of SDBS on the size distribution of iron oxide red

Fig. 9 shows the effect of SDBS on the size distribution of iron oxide red. As shown in Fig. 9, SDBS plays an important role in size distribution of iron oxide particles red. Fig. 9(a) is more monodisperse and regular than Fig. 9(b).

3.5. Nano-iron oxide red product

Characteristics of iron oxide red product prepared under the above optimum conditions (namely phase, sizes and main content) were determined by XRD, LPSA, and Titration. The results

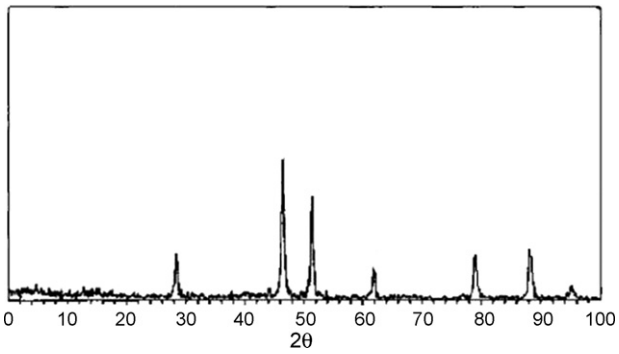

Fig. 10. XRD pattern of iron oxide red product.

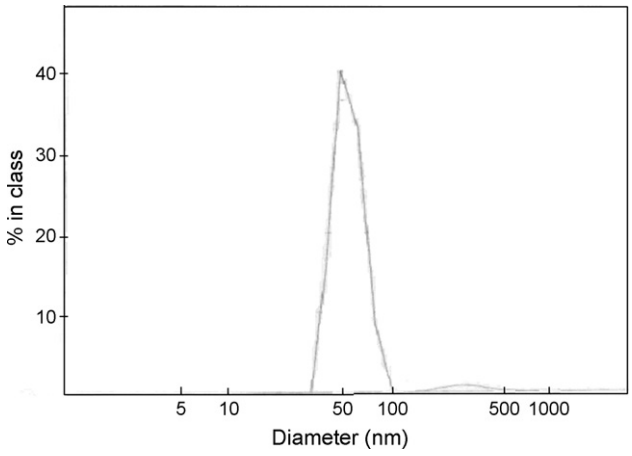

Fig. 11. Size distribution of iron oxide red product.

show that the content of Fe_2O_3 is 92.76%. Fig. 10 shows the XRD pattern of iron oxide red product. It indicates the highly crystalline character of the iron oxide red and matches well with the standard α-Fe_2O_3 (hematite) reflections. Fig. 11 shows the size distribution of iron oxide red product. It was observed that the size of the product is mainly between 40 and 100 nm. This is in accordance with the nano-iron oxide red standard.

4. Conclusions

The experimental results show it is feasible that cyanided tailings were used to prepare red iron oxide pigment via a ammonia process with urea as the precipitant.

At first, cyanided tailings were pretreated. It was found that, under the optimum conditions, arsenic and lead have been removed and pure ferrous sulfate can be gained.

The preparation of seed crystal by the above ferrous sulfate was experimentally investigated. It is obvious that the rate of conversation of ferrous sulfate changes with oxidizing conditions according to the result. The rate of conversation of ferrous sulfate increases with the rise of temperature, velocity of air flow, but decreases with the rise of concentration of ferrous sulfate. On the other hand, seed crystal for preparation of α-Fe_2O_3 must be γ-FeOOH,, otherwise α-Fe_2O_3 can not be obtained.

An ammonia process with urea as the precipitant is successfully used to prepare nano-iron oxide red pigment. The optimum technological parameters are shown below: reaction temperature is 80–85 °C; pH is 3–4; velocity of air flow is 0.14 m^3/h; the molar ratio of urea to ferrous sulfate is 3.5:1; dispersion is added just after adjusting pH. SDBS plays an important role in size distribution of iron oxide red particles and it made regular iron oxide red particles come into being. Under above conditions, we can obtain bright, regular seed crystal and lay a good foundation for preparing excellent nano-iron oxide red pigments. Maybe, this method could be applied into other tailings to prepare pigments.

Acknowledgements

The authors are thankful to the Major project of Educational Ministry (No. 107124), Key Laboratory of Science & Technology of Eco-Textile (Donghua University/Jiangnan University), Ministry of Education, China (ECO-KF-2007-10) and National High Technology Research and Development Program of China (863 Program, No. 2006AA06Z132) for financial support of this study.

References

[1] M.A. Legodi, D. de waal, The preparation of magnetite, goethite, hematite and maghemite of pigment quality from mill scale iron waste, Dyes Pigments 74 (2007) 161–168.
[2] N. Guskos, G.J. Papadopoulos, V. Likodimos, et al., Photoacoustic, EPR and electrical conductivity investigations of three synthetic mineral pigments: hematite, goethite and magnetite, Mater. Res. Bull. 37 (6) (2002) 1051–1061.
[3] P.A. Riveros, J.E. Dutrizac, The precipitation of hematite from ferric chloride media, Hydrometallurgy 46 (1/2) (1997) 85–104.
[4] G. Montes-Hernandez, J. Pironon, F. Villieras, Synthesis of a red iron oxide/montmorillonite pigment in a CO_2-rich brine solution, J. Colloid Interface Sci. (303) (2006) 472–476.
[5] C.Q. Cai, Discussion on real seed during synthesis of ammonium-based iron oxide red, Pant Coat. Ind. 36 (2) (2006) 15–18.
[6] G. Jun-feng, L. Xiaobo, Utilization of cyanided tailings from gold ore dressing plant, Min. Eng. 4 (2005) 38–39.
[7] K.J. Sreeram, R. Indumathy, A. Rajaram, et al., Template synthesis of highly crystalline and monodisperse iron oxide pigments of nanosize, Mater. Res. Bull. (41) (2006) 1875–1881.